Research Square

Preprints are preliminary reports that have not undergone peer review.
They should not be considered conclusive, used to inform clinical practice,
or referenced by the media as validated information.

Impact of uncorrected astigmatism on image quality with dual focus optics - a modelling study

Matt Jaskulski

majask@iu.edu

Indiana University

Arthur Bradley

CooperVision Inc.

Pete Kollbaum

Indiana University

Research Article

Keywords:

Posted Date: May 8th, 2026

DOI: https://doi.org/10.21203/rs.3.rs-9498696/v1

License: This work is licensed under a Creative Commons Attribution 4.0 International License.
Read Full License

Additional Declarations: Competing interest reported. This study was funded by CooperVision, Inc., and AB is an employee of CooperVision, Inc. The research group at Indiana University receives research funding for other projects from Alcon, CooperVision, Essilor, SightGlass Vision, Viatris, and Zeiss.

Impact of uncorrected astigmatism on image quality with dual focus optics - a modelling study

Matt Jaskulski[1], Arthur Bradley[2], Pete Kollbaum[1].

1. Indiana University, Bloomington, United States, School of Optometry
2. CooperVision Inc., San Ramon, United States, Research and Development

Corresponding author: Matt Jaskulski (majask@iu.edu)

Abstract

Purpose: Compare the impact of uncorrected astigmatism in a single vision (SV) and a dual focus (DF) optical model at the center and boundaries of the interval of Sturm.

Methods: With the rule astigmatism (up to 2.00 diopters) was added to a single vision and a dual focus optical model. The dual focus model included an annular zone with +2.00 of added power. For each model, wavefronts were constructed from Zernike polynomials over the full pupil (SV model) or separately (on zone-by-zone basis) in the DF model. Geometric ray tracing and wave optics were used to compute point-spread functions (PSFs), Modulation Transfer Functions (MTFs) and simulated letter images at the center and anterior and posterior ends of the "Interval of Sturm" (IOS).

Results: Simple line foci were observed with the SV model, but more complicated PSFs containing circular, elliptical and double orthogonal line components were created when astigmatism was added to the DF model. Simulated images in both the SV and DF models were degraded with increasing levels of astigmatism. In the absence of astigmatism, lens only MTFs were reduced by approximately 50% in the DF model, but as astigmatism levels increased, MTF values and differences in MTFs between the SV and DF models were reduced. In the presence of ocular aberrations MTFs with astigmatisms greater than 1.00D were almost identical in the SV and DF models.

Conclusions: The modeling shows that uncorrected astigmatism remains a major contributor to image degradation in eyes corrected with a DF contact lens suggesting that astigmatic eyes fit with dual focus myopia control contact lenses would benefit from a toric correction.

Introduction

Following Thomas Young's description of his own refractive astigmatism in 1800, mathematician and astronomer William Airy corrected the astigmatism in his left eye with a cylindrical lens in 1825.[1] There are two general sources of refractive astigmatism in the human eye; one caused by toricities in the cornea or lens, and the other due to e.g. the visual axis being tilted relative to the optical axis (in which case the foveally-measured astigmatism will include off-axis, oblique astigmatism).[2,3] Astigmatism includes a meridional variation in refractive states wherein the (orthogonal) vertical and horizontal meridians exhibit maximum and minimum powers, creating the common with- and against-the-rule (WTR and ATR) astigmatic refractive errors.[4,5] WTR being more prevalent in younger eyes.[6,7]

Prevalence of astigmatism in human eyes varies with age,[8] presence of myopia,[5,9,10] and ethnicity.[10,11,12] Astigmatism lesser than 1.00 D is the most common,[5,7] but between 20 and 40% of adult eyes have 1.0 D or more of refractive astigmatism, [8,11,13] and prevalence levels can rise to 70% - 87% of eye clinic populations.[6,7]

Uncorrected refractive astigmatism creates perpendicular elongated point-spread functions (PSF) at each end of the focal interval (the "Interval of Sturm", IOS), and a non-meridionally biased blurred PSF at the center of this power range (the "circle of least confusion", which can resemble a square rotated 45 degrees).[14] Uncorrected astigmatism reduces visual acuity[15,16] and contrast sensitivity,[17] slows reading speed,[18] impairs driving performance,[19,20] and can induce monocular diplopia[21,22,23] or create blur that can be subjectively troublesome and objectionable.[24] The visual impact of uncorrected astigmatism becomes evident for levels of astigmatism greater than or equal to 0.50D.[25,26,26,28] Refractive corrections for astigmatism are available in contact lenses[29] and spectacles. Read et al. provides a comprehensive review of astigmatism and its visual impact.[30]

Although increasing levels of uncorrected astigmatism create a monotonic increase in retinal blur with associated decreases in visual acuity and contrast sensitivity,[17,31,32] the presence of uncorrected astigmatism in retinal images generated by multifocal intra-ocular lenses (IOLs) can result in complex PSFs that vary both radially and meridionally.[33] Some evidence suggests that the presence of one aberration can minimize the impact of another,[34] raising the possibility that eyes fit with myopia control or aberrated multifocal lenses may not require correction for astigmatism. However, experimental studies of pseudophakic eyes show that vision consequences of uncorrected astigmatism are similar[35,36] or even greater[37] in eyes fit with multifocal IOLs compared to eyes fit with single vision IOLs.

The aim of this modelling study is to explore the consequences of uncorrected astigmatism on retinal image quality with dual focus (DF) contact lenses. Uncorrected astigmatism in an eye

corrected with a DF contact lens creates a refractive error that varies both radially and meridionally. Will uncorrected astigmatism degrade image quality when an eye is corrected with a DF myopia control lens? Also, will astigmatism correction benefit astigmatic patients fit with dual focus myopia control contact lenses? Given the zonal, discontinuous nature of dual-focus optics, a combined modal–zonal modeling approach enabled quantitative investigation of these questions.

Methods

Sign conventions

Throughout this manuscript spherical wavefronts are expressed as having wavefront vergence in diopters where positive and negative dioptric values describe converging and diverging wavefronts, respectively. Therefore, positive dioptric values are used to describe the converging wavefront exiting a myopic eye, which is contrary to clinical convention in which myopia is defined by the negative powered lenses used for its correction. The model included +2.00 D of excess power in the vertical meridian (WTR astigmatism, Rx plano -2.00 x 180), and +2.00 D of add power in an annular treatment zone of the DF myopia control lens.

The modeled optics

A schematic geometrical optics illustration of light deviations due to uncorrected astigmatism in single vision (SV) and DF optics are shown in Figure 1. A reference model (top left) without astigmatism or zonal optics exhibits a single focal plane and a point PSF. In the presence of uncorrected astigmatism such as WTR astigmatism (bottom left, wherein the eye has added optical power along the vertical meridian) the single focal plane is split into an “Interval of Sturm” wherein the added power in the vertical meridian creates a horizontal “line focus” (focused vertically, blurred horizontally) anterior to the focal plane at which the PSF is a vertical line (focused horizontally, blurred vertically), being created by the other (horizontal) meridian.

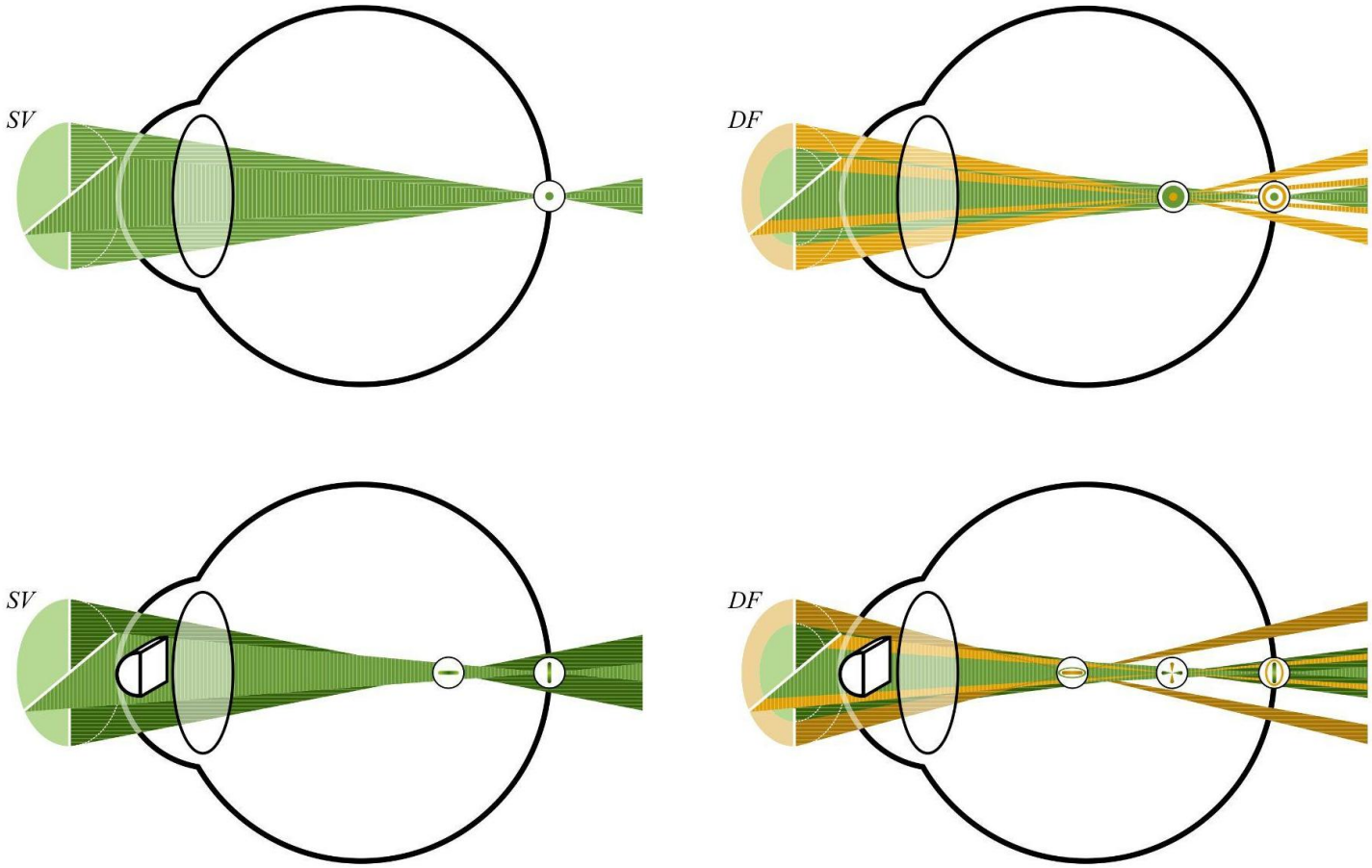


Figure 1. A simplified geometrical optics illustration of light deviation with and without WTR astigmatism in combination with SV (left column) and DF (right column) optics. The presence of WTR astigmatism (bottom row) is represented with the convex cylinder symbol. Horizontal and vertical meridians are represented with solid white lines inside the schematic wavefront ovals on the left of each diagram. In the DF model, light rays from the distance and treatment optics are represented in green and yellow, respectively. Dark and light colors represent light rays corresponding to the more and less myopic meridians, respectively. The small circles located at the foci represent the borders of the interval of Sturm and the symbols inside represent the simplified shapes of PSFs expected at the corresponding focal planes.

Without astigmatism, the DF optic produces a composite PSF (top right) at the distance correction focal plane including a distance-optic generated central PSF core surrounded by a blur ring generated by the annular treatment zone which focuses anteriorly with respect to the distance correction optic focal plane. When both astigmatism and dual focus optics are present (bottom right) two intervals of Sturm exist: one created by the distance- and another by the treatment optic. If the optical power differences due to astigmatism are of the same magnitude as the added plus power of the treatment optic (e.g. 2.00 D in the current model), the most anterior IOS edge created by the distance optic will coincide with the least anterior edge of the interval created by the treatment optic. At that plane, the resulting PSF becomes a combination of vertical and horizontal line foci.[33]

Data processing - modelling lenses with wavefronts

Optical modelling used custom software (Indiana Wavefront Analyzer – IWA, Maple, LLC, mapleoptics.com, implemented in Matlab, mathworks.com). Optics containing defocus, astigmatism, zonal geometry and ocular aberrations were defined as wavefront errors across the full pupil (SV model) or separately across each individual zone (DF model) from which the following were derived:

- Wavefront slope *(δW/δr)* – for every point in the pupil it defines the ray deviation angles which are measured by aberrometers.[38]

- Wavefront vergence: *(δW/δr)/r* – for every point in the pupil it describes the optical power (in diopters) defined by the position along the optical axis of intersections between it and each ray.[39] In case of a simple lens, this is commonly referred to as the "optical power" and for an eye, vergence of the exiting wavefront is a measure of the local refractive error.

Sphero-cylindrical clinical prescriptions for the uncorrected astigmatism to be induced were first converted into the power vector space M, J0 and J45, and then into a normalized Zernike vector using equations by Thibos et al.[40]

- Geometrical optics PSFs were generated by propagating the pupil-plane wavefronts forward to the image plane and then computing ray density histograms. These PSFs reflect all the refractive properties of the lenses but lack the wave phenomena (diffraction or interference).[39]

- Fourier optics PSFs which include these wave phenomena were computed as the squared magnitude of the Fourier transform of the generalized pupil function, defined by the amplitude phase of the wavefront:

$$P(x,y) = A(x,y) \cdot exp(\frac{i2\pi W(x,y)}{\lambda}) \quad (1)$$

where: *W(x, y)* is the wavefront error, *A(x, y)* is the amplitude function (which equaled 1 but can generally be used to model the Stiles Crawford Effect, cataracts, etc.) and λ is the wavelength. These PSFs include the wave effects and have been experimentally confirmed to closely match the physical world.[41,42] After their computation, the Fourier PSFs were scaled according to the pupil diameter.

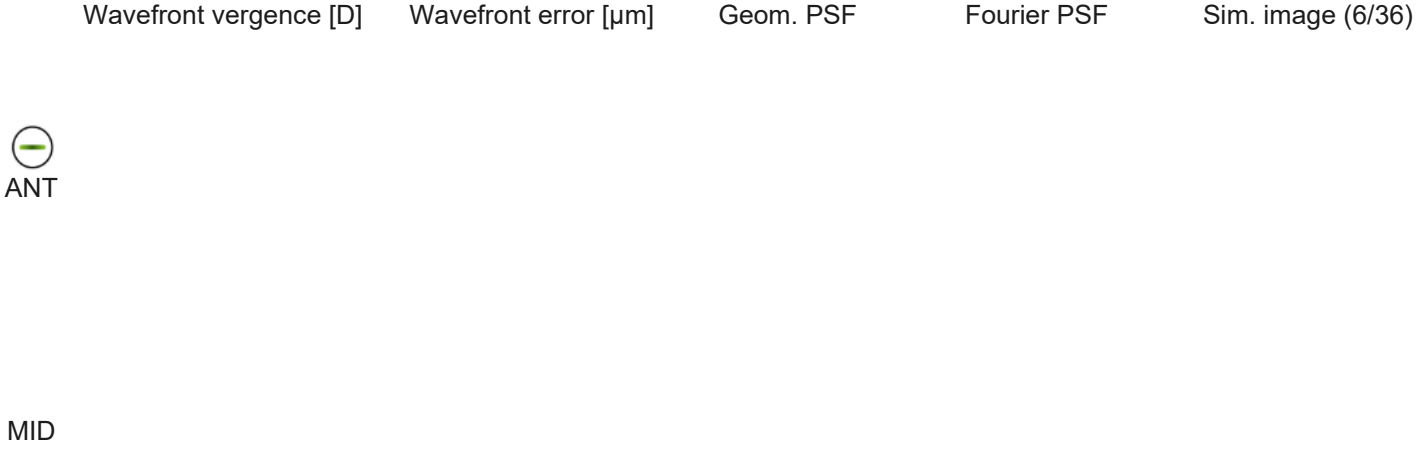
$$f_c = \frac{\varnothing}{\lambda} \cdot \frac{\pi}{180} \quad (2)$$

where: f_c is the cutoff frequency (bandwidth) in cycles per degree, $\emptyset$ is the measurement aperture diameter (4.8 mm or 6.0 mm) and λ is the measurement wavelength (540 nm).

Simulated retinal images of 30 arc minute (6/36) letter E's were calculated using the inverse Fourier transform of the product of the Fourier-transformed PSFs and optotype images. This method is effectively the same as a spatial-domain convolution between a PSF and image, but much faster to compute. Modulation transfer functions (MTFs) were obtained by taking the absolute value of the OTFs. Because OTFs and MTFs are fundamentally two-dimensional functions of spatial frequency coordinates, radial averages were calculated to reduce them to one-dimensional functions of modulation vs spatial frequency. MTFs were calculated for models of lens-only optics (including astigmatism, diffraction and zonal geometry in the DF model) and lens-plus-ocular-aberrations (high order aberrations HOA for a typical young adult eye listed in Table 1 in the Appendix).

Results

Pupil- and image-plane properties of the astigmatic model (6.0 mm pupil diameter) are shown in Figures 2 and 3 for the modeled SV and DF optics, respectively. Both models include +2.00 D of vertical meridian defocus (axis 180, WTR astigmatism, clinical refractive correction of plano -2.00 x 180). The DF model included an annular ring containing +2.00 D of added power. Each of the columns 1-5 describe, respectively, wavefront vergence maps (defocus), 3D projections of wavefront errors, geometric PSF, wave optics PSF, and simulated images of a 6/36 high contrast letter E's. The top, middle, and bottom rows represent optics and images when the anterior end, center and posterior end of the Interval of Sturm (IOS) has been focused (by adjusting spherical defocus with Z20).



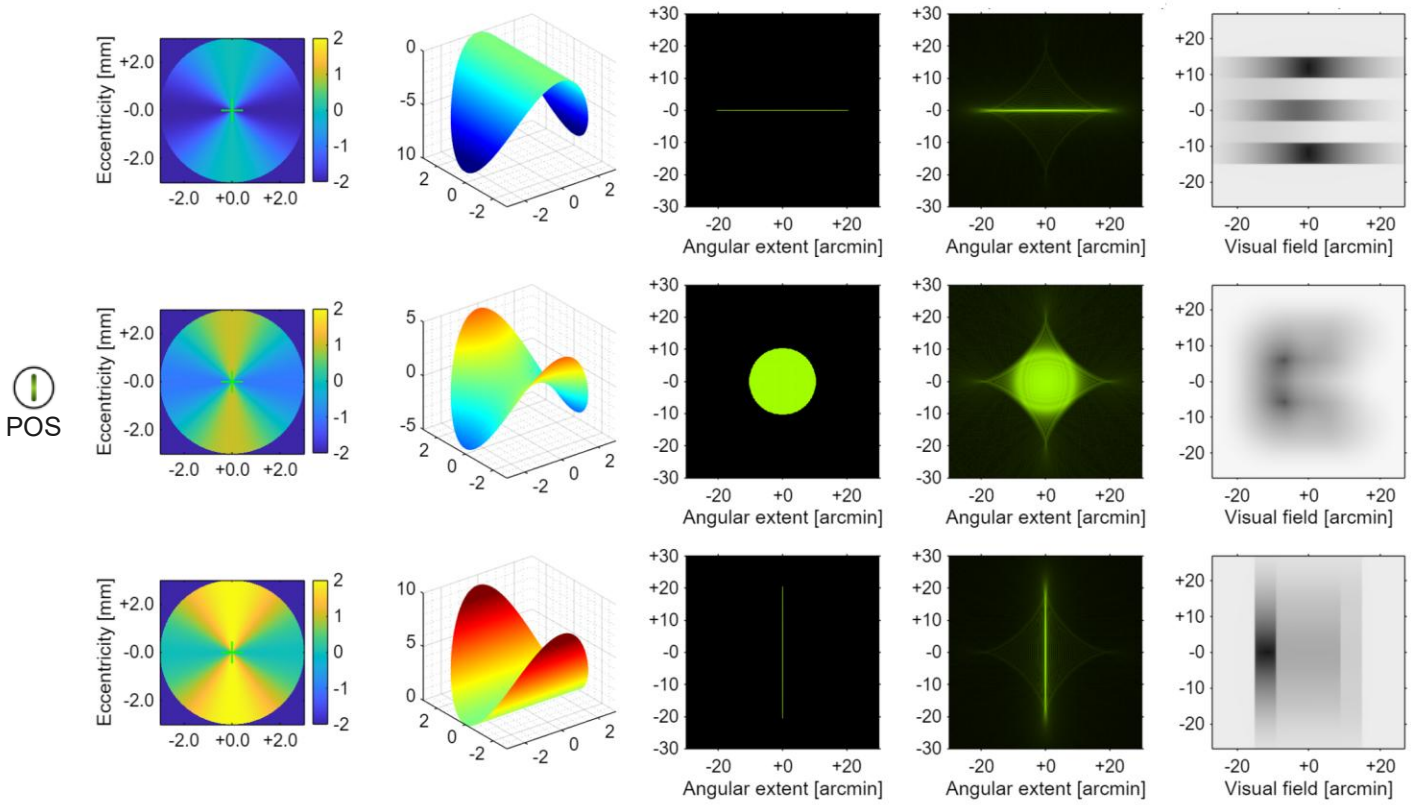


Figure 2. Example pupil- (columns 1, 2) and image-plane (columns 3 - 5) descriptors of the SV lens astigmatic model (+2.00 D of optical power added along the vertical meridian for a 6.0 mm pupil). The row labels include symbols shared with Figure 1 ("ANT", "MID", and "POS") which indicate the plane within the Interval of Sturm being modeled. Wavefront vergence and errors are plotted as a function of pupil location in mm. PSFs, and simulated images are shown in image coordinates of arc minutes.

The impact of uncorrected astigmatism was also evident in the wavefronts, PSFs and simulated images created by the DF model (Figure 3). For example, at the anterior edge of the IOS for the distance correction, the axis 180 astigmatism showed a line focused vertically and blurred horizontally, while the annular treatment optic had its least positive meridian focused creating a line focused horizontally and blurred vertically, together creating a cross PSF. For more posterior planes (center and posterior end of the IOS for the distance correction) the blur created by the treatment zone increased creating a vertical oval pattern. At the center of the IOS of the distance correction the center zone and outer annulus of the distance optic created a PSF including circle surrounded by a circular annulus.



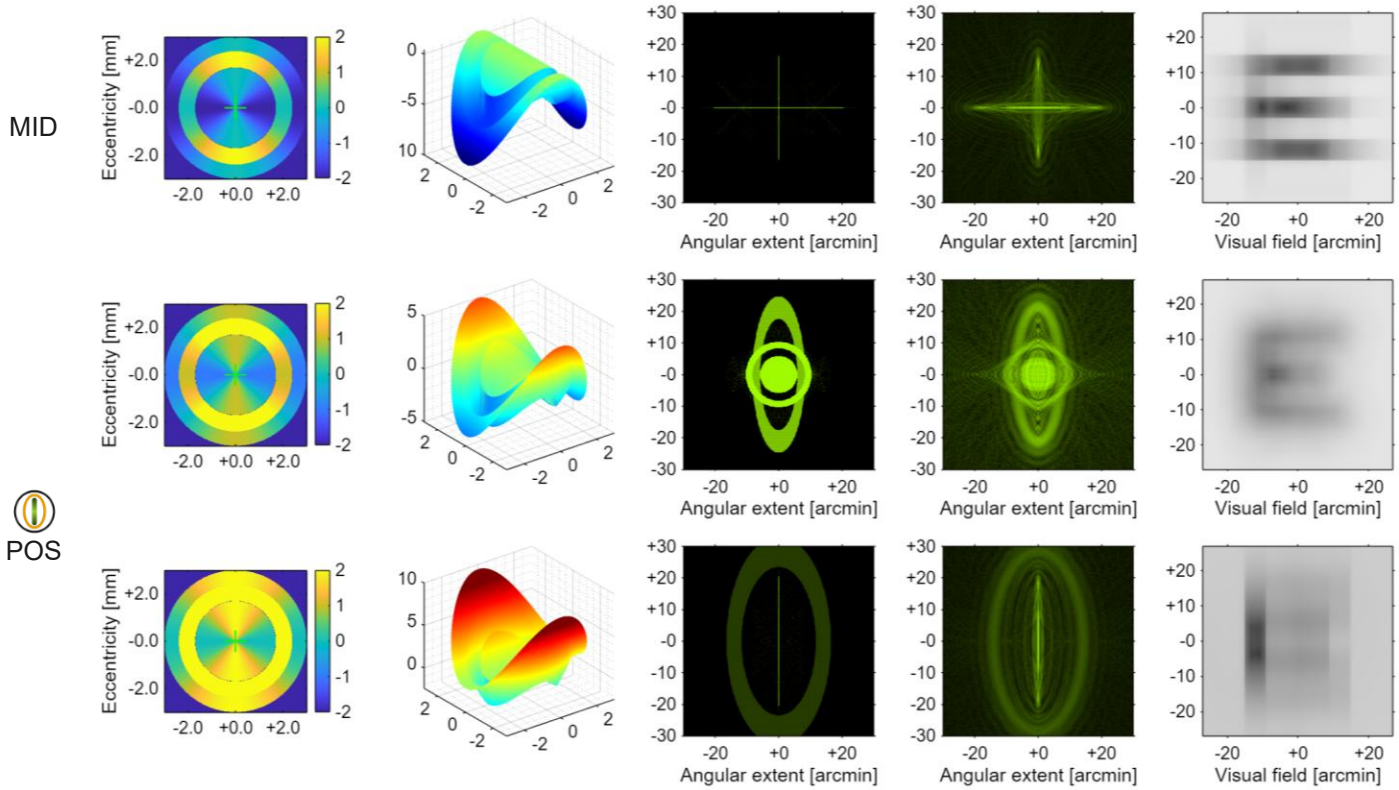
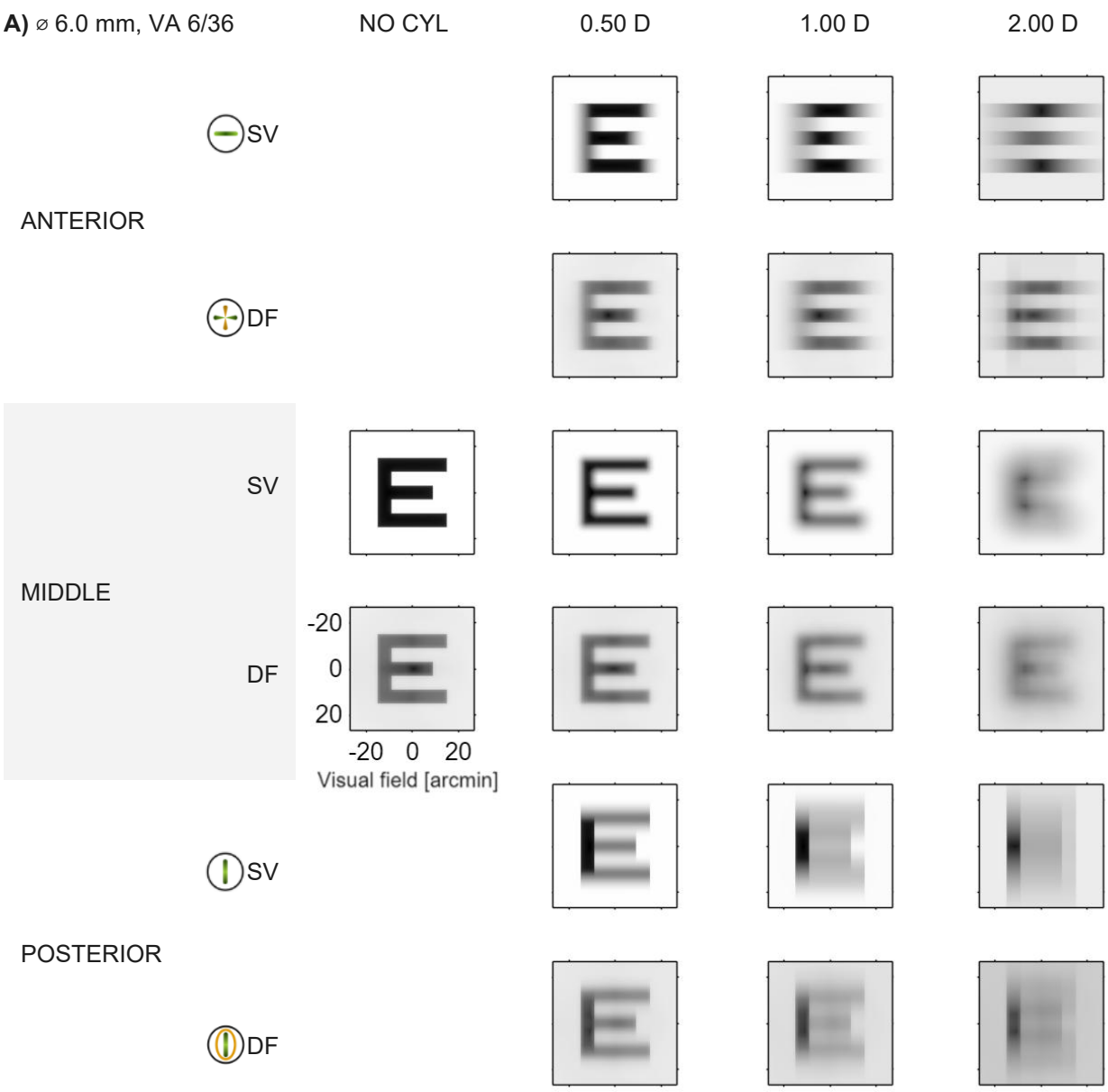


Figure 3. Examples of the pupil- (columns 1, 2) and image-plane (columns 3 - 5) descriptors of the DF lens model (+2.00 D of optical power added along the vertical meridian and +2.00D of added power in the annular ring for a 6.0 mm pupil). The three rows represent the planes within the distance correction interval of Sturm. Wavefront vergence and errors are plotted as a function of pupil location in mm. PSFs, and simulated images are shown in image coordinates of arc minutes.

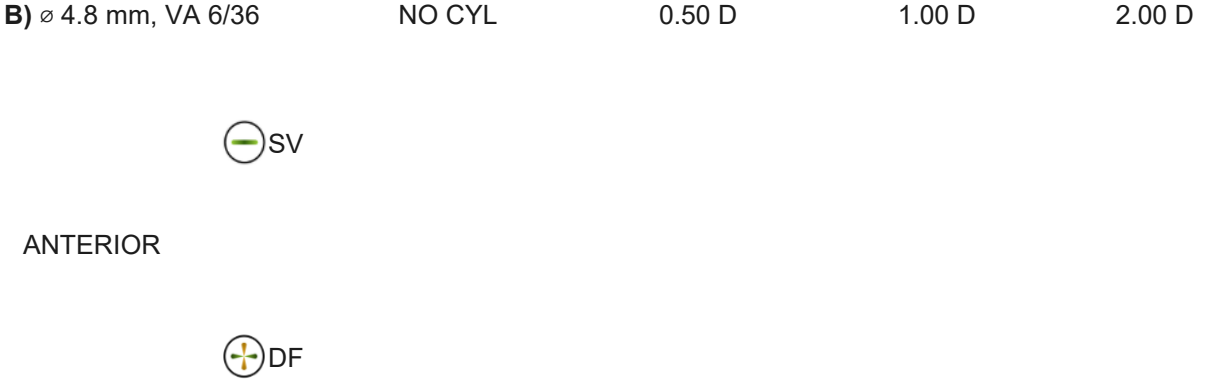
In both models, the simulated letter E exhibited a clear focus of horizontal and vertical contours at the anterior- and posterior end of the IOS, respectively. Neither vertical nor horizontal contours were focused on the center of the IOS. Consistent with the cross PSF present at the anterior edge of the distance optic IOS in the DF model (Figure 3), the simulated E included both focus and blur in horizontal and vertical contours.

Figures 4 A & B show side-by-side comparisons of simulated retinal images (6/36 Snellen E) for modeled SV and DF optics at different planes within the IOS for 3 levels (0.50, 1.00 and 2.00 D) of astigmatism and two pupil diameters (6.0 mm and 4.8 mm). In the case of the 6.0 mm pupil, the modeled DF optic included the central zone distance correction, the first treatment annulus and a part of the second distance correction annulus, whereas the 4.8 mm pupil included only the central distance correction optical zone and the first treatment annulus. Evidence of two-meridian blur combined with two-meridian focus can be seen in the DF model at the anterior edge of the distance correction IOS. The all-meridian blur is present at the center of the IOS for both models, but more visible for the SV model. The vertical blur demodulates horizontal contours at the posterior edge of the IOS for both models, but less so for the DF model.

1


A) ⌀ 6.0 mm, VA 6/36
NO CYL
0.50 D
1.00 D
2.00 D
SV
ANTERIOR
DF
SV
MIDDLE
DF
-20
0
20
-20 0 20
Visual field [arcmin]
SV
POSTERIOR
DF

2


B) ⌀ 4.8 mm, VA 6/36
NO CYL
0.50 D
1.00 D
2.00 D
SV
ANTERIOR
DF

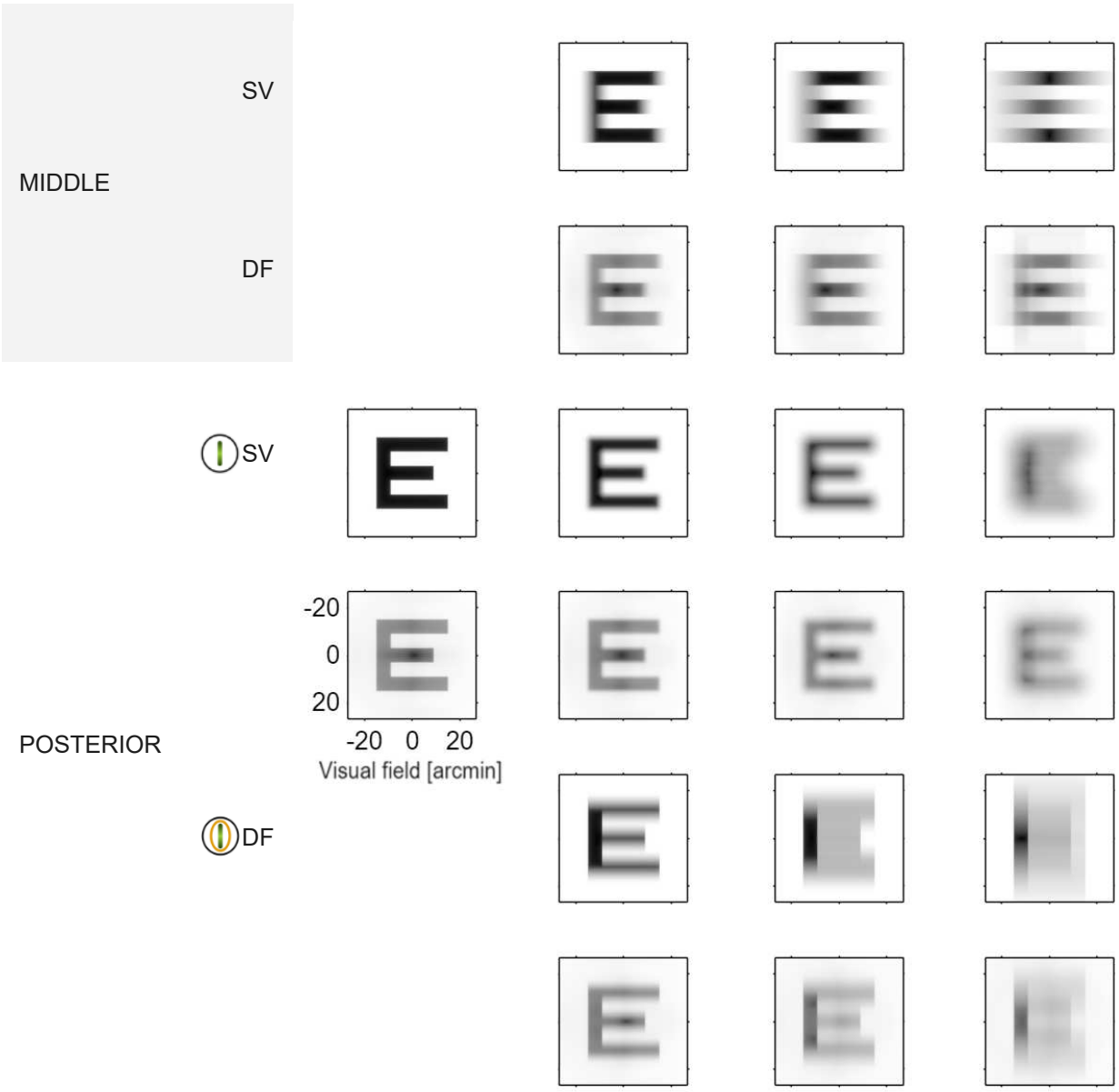
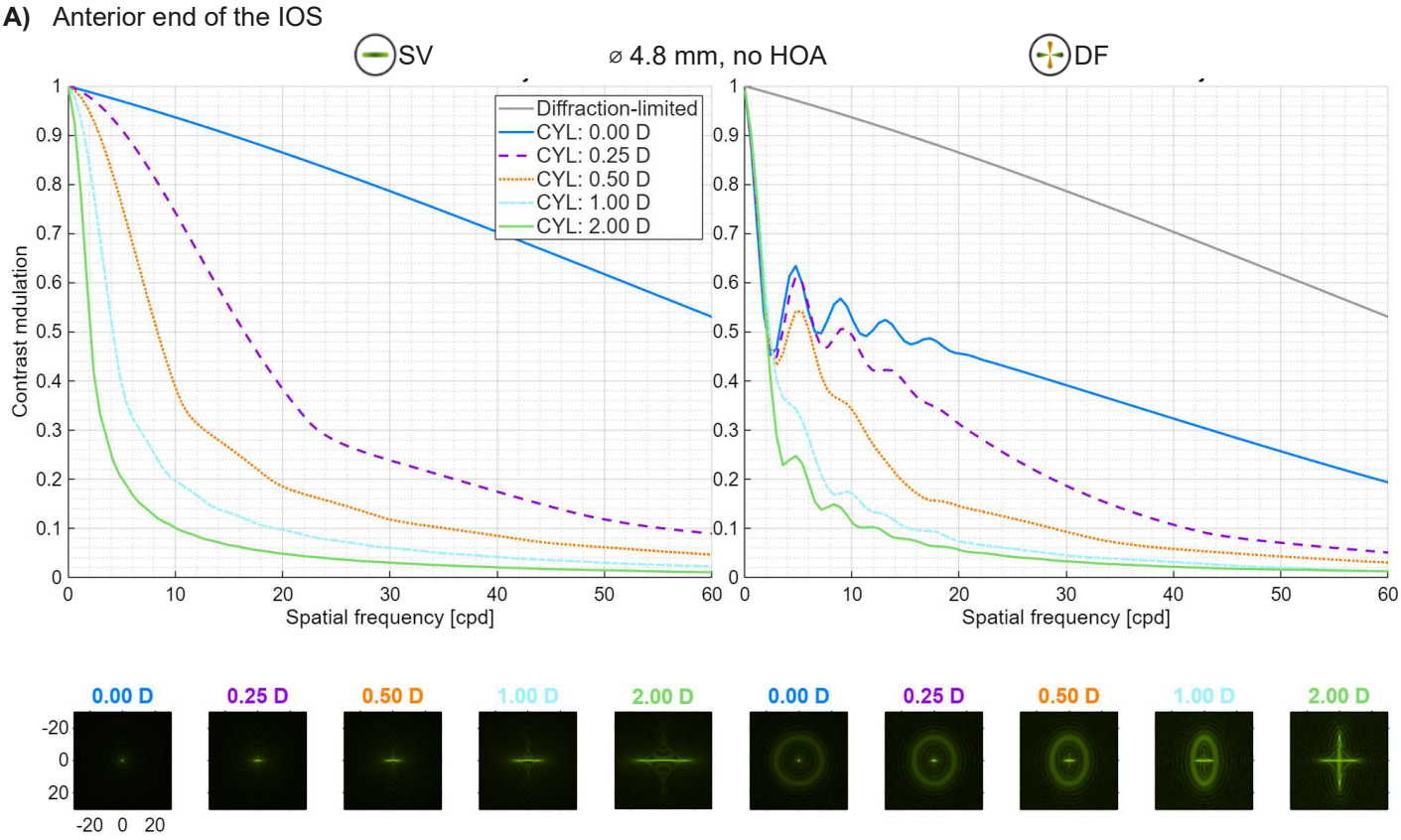


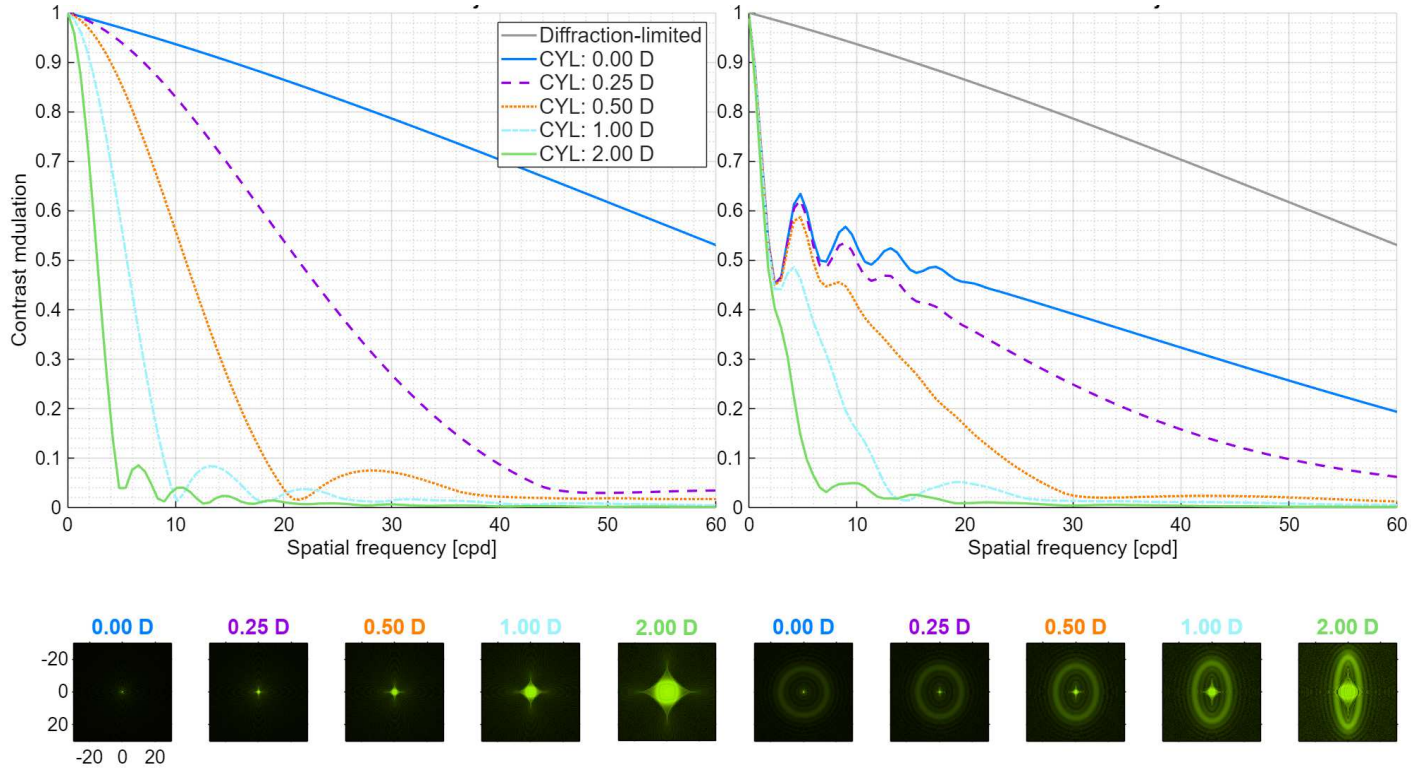
Figure 4. Simulated retinal images for the modeled SV and DF optics for different planes of focus within the IOS (rows) and magnitudes of cylinder (columns). The modeled pupil diameter was A) 6.0 mm and B) 4.8 mm, and the Snellen E size was 30 arc minutes (6/36).

Radially averaged MTFs provided quantitative assessments of the impact of varying magnitudes of uncorrected astigmatism for the SV and DF models for each plane within the IOS. Figure 5 compares the MTFs for the SV (left) and DF (right) for the three focal planes (A-C) with 5 levels of astigmatism (0.00, 0.25, 0.50, 1.00, 2.00 D) for a 4.8 mm pupil diameter. The MTFs in Figure 5 reflect the lens-only optics, whereas the MTFs in Figure 6 reflect the combined impact of lens optics and ocular aberrations (see Table 1 in Appendix).

In the absence of astigmatism, the SV lens-only MTF is diffraction limited and the DF lens-only MTF drops to approximately 50% of the SV diffraction-limited values beyond about 10 cpd because only ~50% of the light is focused (the other ~50% being defocused by the treatment

optic). MTF values steadily decline as astigmatism increases in both SV and DF models. The differences between SV and DF MTFs become much smaller once uncorrected astigmatism is introduced into the model. For example, with zero astigmatism, MTFs at 20 cpd are 0.86 and 0.46 respectively in the SV and DF models, and with 0.50 D of astigmatism the MTFs drop to more similar values of 0.19 and 0.15 at ends of the IOS. At the center of the IOS, MTF values at low SFs remain generally higher for the SV model, but the DF model has higher MTF values at higher SFs. For each astigmatism level, the differences observed between the lens only SV and DF models generally become much smaller after ocular HOAs are included (Figure 6).





C) Posterior end of the IOS

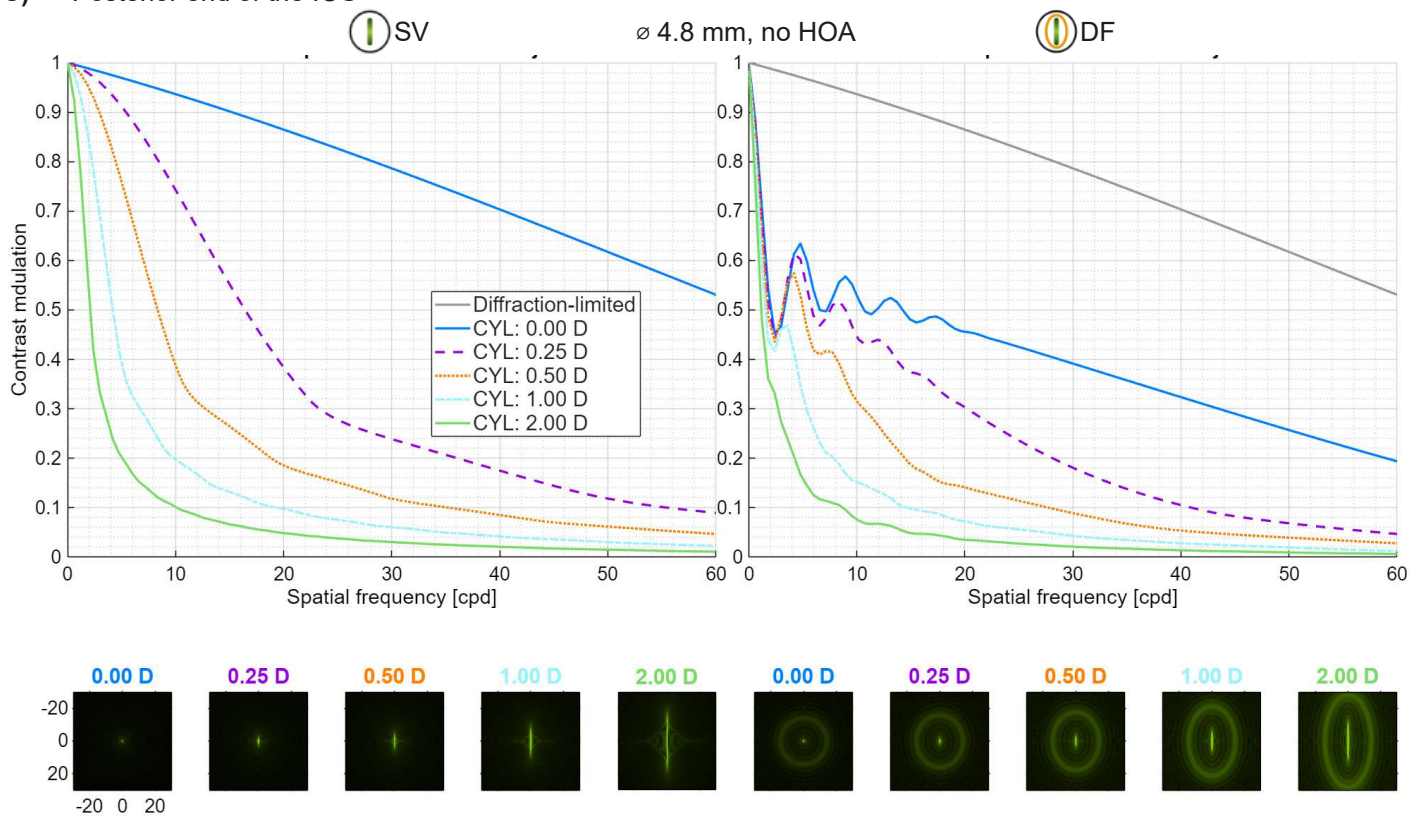
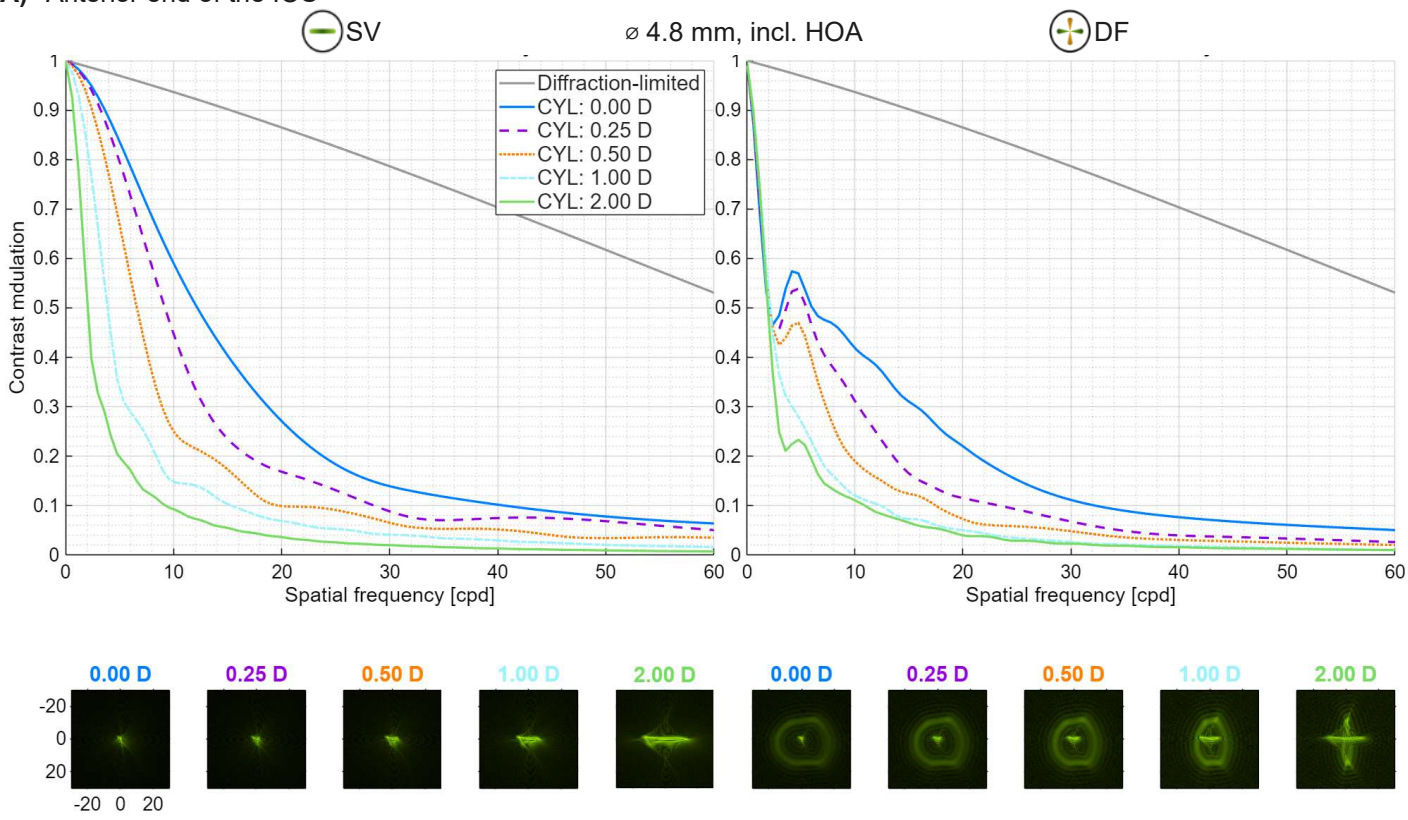
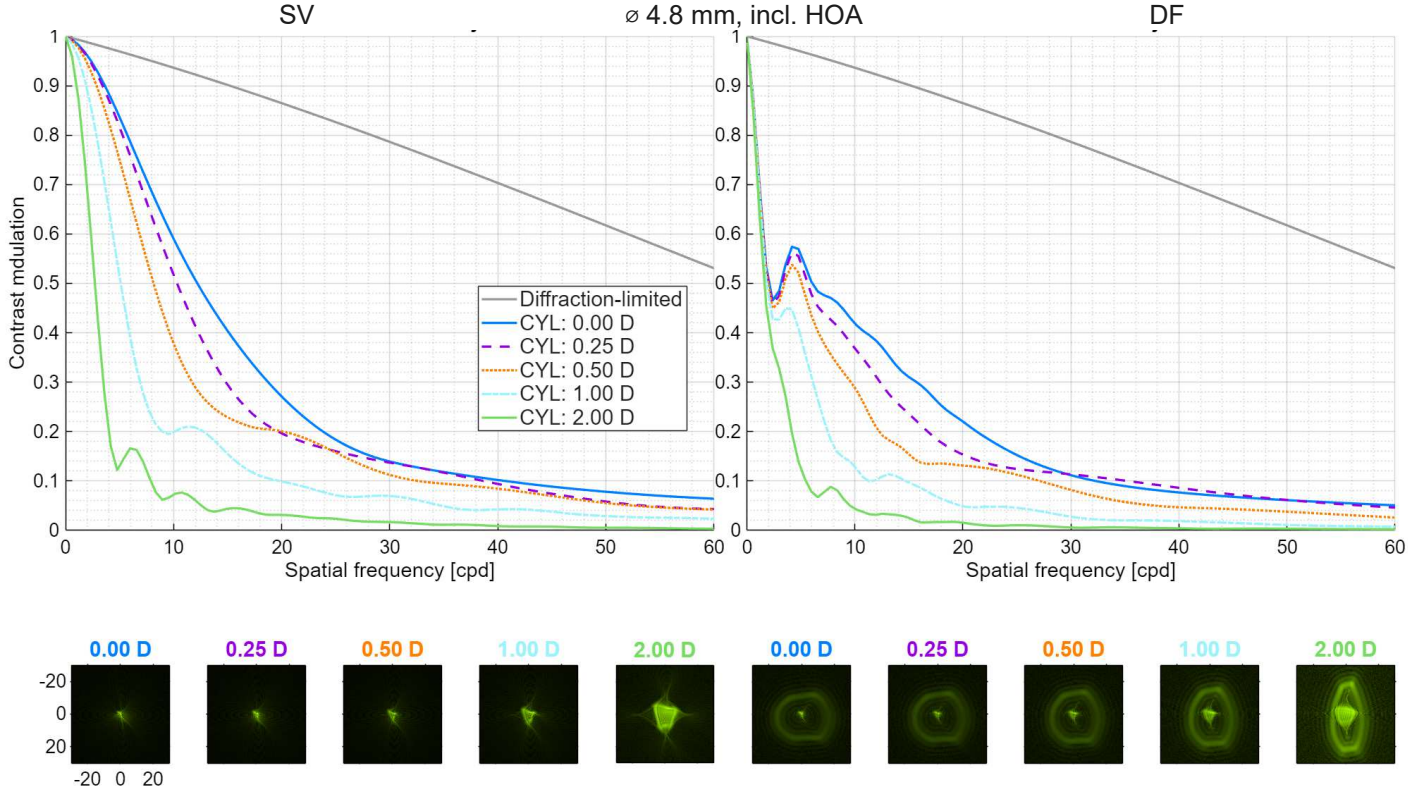


Figure 5. Radially averaged MTFs (top) and Fourier PSFs (bottom) for the SV (left) and DF (right) models for different magnitudes of cylinder (colored data series), and planes of focus within the IOS (A - C). The model used 4.8 mm pupils and included only defocus and astigmatism aberration terms generated by each model (no higher order aberrations).

A) Anterior end of the IOS



B) Middle of the IOS



C) Posterior end of the IOS

SV ⌀ 4.8 mm, incl. HOA DF

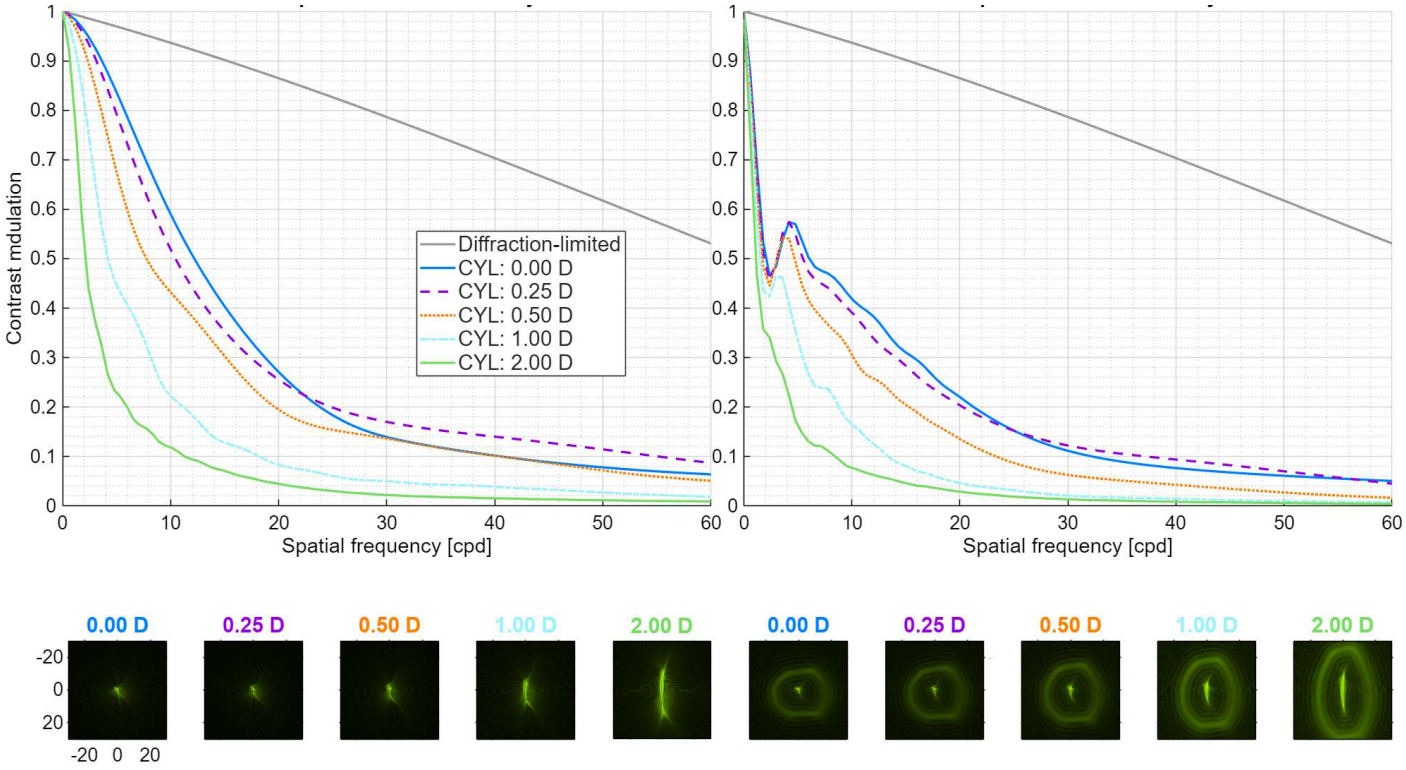


Figure 6. Radially averaged MTFs (top) and Fourier PSFs (bottom) for the modeled SV (left) and DF (right) optics for different magnitudes of cylinder (colored data series), and planes of focus within the IOS (A - C). The model used 4.8 mm pupils and included HOAs of a typical young adult eye (see Table 1 in Appendix).

To facilitate the comparison of the effects of uncorrected astigmatism on the SV and DF models with and without ocular aberrations, MTF values at 8 and 15 cpd are plotted as a function of increasing magnitudes of uncorrected astigmatism for the three planes within the IOS for all 4 models (Figure 7). The decrease in image modulation generated by adding ocular HOAs is highly significant in the absence of astigmatism, but mostly disappears once astigmatism levels are ≥1.00 D. Similarly, MTF differences between SV and DF models when no astigmatism is present also mostly disappear with astigmatisms greater than 1.00 D.

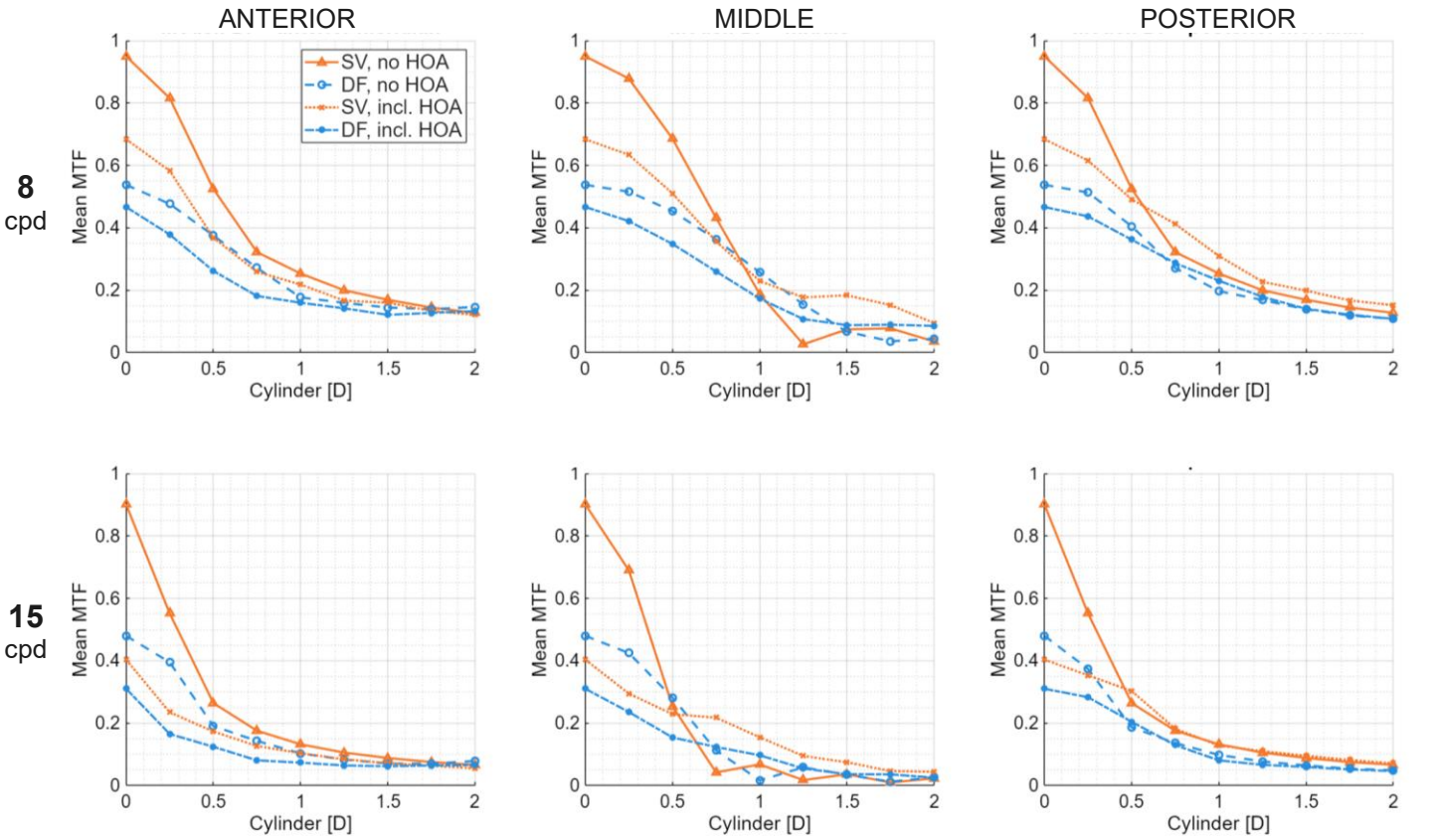


Figure 7. Mean radial average MTF values for 8 and 15 cycles per degree for the SV (top row) and DF (bottom row) models, for the three planes of the IOS (columns 1 - 3). The model used 4.8 mm pupils and shows the values for models with (blue) and without (orange) added ocular HOAs.

Discussion

Optical modeling revealed that uncorrected astigmatism had a readily observable impact on image quality in both the SV and DF lens-only models (Figures 2-4), which were quantified with radially averaged MTFs (Figure 5 and 6). The length of geometrical optics PSF line foci at the edge of the IOS can be predicted for the SV model to be 41 arc minutes due to the 2.00 D of meridional defocus and the 6.0 mm pupil:[43]

$$B = K \cdot \varnothing \cdot D \tag{3}$$

where B - blur diameter in arc minutes, K - unit scaling constant 3.42, $\varnothing$ - pupil diameter in mm, D - defocus in diopters.

At the center of the IOS, where defocus levels are half those at the edges, a circular blur patch with a diameter of 20.5 arc minutes is generated. Similarly, the same equation can be used to estimate the diameter of the blur patterns generated by a +2.00 D add ring in the DF model. For

example, at the plane where the most myopic meridian of the distance correction is focused, the least myopic meridian of the treatment optic was also focused generating two orthogonal line foci (Figure 3), one generated by 2.00 D of defocus across the 6.0 mm pupil and one 2.00 D of defocus across a 4.8 mm diameter annulus resulting in a cross that is 41 arc minutes horizontally and 33 arc minutes vertically. In this unique scenario, the resulting images have one meridian focused by the distance correction optic and the perpendicular meridian focused by the treatment optic (see simulated images for DF model at the anterior edge of the IOS in Figures 3 and 4). Similar crossed images were observed experimentally when adding astigmatism to a multifocal model.[14]

The simulated retinal images of optotype E's (Figure 4) reveal that DF focus optics lower image contrast, and that in the presence of 2.00 D of astigmatism images at the anterior end and center of the IOS contain light focused at both horizontal- and vertical meridians (see discussion above), enabling both horizontal and vertical contours in the image to appear focused. The reduced blur at the center of the IOS observed in the DF images with 2.00 D of astigmatism reflects the smaller distance optic CZ (3.3 mm diameter) being defocused by ~1.00 D relative to the 6.0 mm and 4.8 mm diameters in modeled SV optics. Equation 3 predicts this, showing that defocus blur will scale with aperture size. This calculation highlights the concept of a "virtual pinhole" created when only a small central region is involved in generating the distance image (while the surrounding optic is defocused or highly aberrated). Although reducing the center-zone will reduce blur from any uncorrected astigmatism and thus expand the depth of focus, reducing the size of the distance correction optic will also lower image contrast.[44] Such virtual pinholes, therefore, reduce the impact of but do not correct the astigmatism and are accompanied by generally lowered image contrasts.

The lens-only model (Figure 5) creates a monotonic decline in contrast with increasing levels of astigmatism in both the SV and DF models. At low spatial frequencies (lower than 3 cpd) image modulation in the DF model is dominated by the contrast lowering effects of the dual focus optics, but at frequencies greater than 3 cpd, additional decreases in contrast are created by uncorrected astigmatism. The expected large difference in MTFs for the SV and DF models with zero astigmatism (Figure 5) became more similar when the aberrated eye optics were added to the model (Figure 6). With levels of astigmatism ≥1.00 D the image contrasts in the SV and DF models were almost the same in the presence of ocular HOAs (Figure 7).

If the need to correct astigmatism is based upon the relative reduction in image quality, eyes with SV corrections may require corrections for lower levels of astigmatism. However, if the need for a toric correction occurs when astigmatism causes image quality to drop below some criterion level (e.g. that needed to read standard text), the need for toric corrections may occur with the same astigmatism magnitude in eyes with SV or DF corrections because the MTF values observed in the SV and DF models with astigmatism ≥1.00D and ocular HOAs are very similar (Figure 7).

Experimental studies showing that uncorrected astigmatism has similar detrimental visual effects in eyes with multifocal corrections as observed in eyes with SV corrections[35,36,45,46] are consistent with astigmatism corrections being driven by resulting absolute image quality.

The present modelling suggests that eyes fit with DF lenses (as used for myopia control) should not be expected to be immune from the detrimental effects of uncorrected astigmatism. Accordingly, these findings suggest that astigmatic eyes fitted with dual-focus contact lenses can derive visual benefits from toric correction comparable to astigmatic eyes fit with single vision corrections.

References

1. Grzybowski A. Beginnings of astigmatism understanding and management in the 19th century. Acta Ophthalmologica. 2015;93(4):e275–e276. doi:10.1111/aos.12684.
2. Liu, Tao, and Larry N. Thibos. "Interaction of axial and oblique astigmatism in theoretical and physical eye models." Journal of the Optical Society of America A 33.9 (2016): 1723-1734.
3. Liu, Tao, and Larry N. Thibos. "Variation of axial and oblique astigmatism with accommodation across the visual field." Journal of Vision 17.3 (2017): 24-24.
4. Kruse, A., & Løfstrøm, T. (1996). How much visual benefit does an astigmat achieve being corrected with a toric correction? International Contact Lens Clinic, 23(2), 59-66.
5. Young G, Sulley A, Hunt C. Prevalence of astigmatism in relation to soft contact lens fitting. Eye & Contact Lens. 2011
6. Luensmann D, Schaeffer JL, Rumney NJ, Stanberry A, Fonn D. Magnitude of astigmatism - A comparison between eyes. Cont Lens Anterior Eye. 2022 Oct;45(5):101510. doi: 10.1016/j.clae.2021.101510. Epub 2021 Sep 7. PMID: 34507898.
7. Nemeth G, Szalai E, Berta A, Modis L Jr. Astigmatism prevalence and biometric analysis in normal population. Eur J Ophthalmol. 2013 Nov-Dec;23(6):779-83. doi: 10.5301/ejo.5000294. Epub 2013 Apr 29. PMID: 23640506.
8. Pärssinen O, Kauppinen M, Viljanen A. Astigmatism among myopics and its changes from childhood to adult age: a 23-year follow-up study. Acta Ophthalmol. 2015 May;93(3):276-83. doi: 10.1111/aos.12572. Epub 2014 Nov 11. PMID: 25384542.
9. Kaye SB, Patterson A. Association between total astigmatism and myopia. J Cataract Refract Surg. 1997 Dec;23(10):1496-502. doi: 10.1016/s0886-3350(97)80020-x. PMID: 9456407.
10. Tong L, Saw SM, Lin Y, Chia KS, Koh D, Tan D. Incidence and progression of astigmatism in Singaporean children. Invest Ophthalmol Vis Sci. 2004 Nov;45(11):3914-8. doi: 10.1167/iovs.04-0492. PMID: 15505036.

11. Kleinstein RN, Jones LA, Hullett S, Kwon S, Lee RJ, Friedman NE, Manny RE, Mutti DO, Yu JA, Zadnik K; Collaborative Longitudinal Evaluation of Ethnicity and Refractive Error Study Group. Refractive error and ethnicity in children. Arch Ophthalmol. 2003 Aug;121(8):1141-7. doi: 10.1001/archopht.121.8.1141. PMID: 12912692.
12. Rim TH, Kim SH, Lim KH, Choi M, Kim HY, Baek SH; Epidemiologic Survey Committee of the Korean Ophthalmological Society. Refractive Errors in Koreans: The Korea National Health and Nutrition Examination Survey 2008-2012. Korean J Ophthalmol. 2016 Jun;30(3):214-24. doi: 10.3341/kjo.2016.30.3.214. Epub 2016 May 18. PMID: 27247521; PMCID: PMC4878982.
13. Vitale S, Ellwein L, Cotch MF, Ferris FL 3rd, Sperduto R. Prevalence of refractive error in the United States, 1999-2004. Arch Ophthalmol. 2008 Aug;126(8):1111-9. doi: 10.1001/archopht.126.8.1111. PMID: 18695106; PMCID: PMC2772054.
14. Sawides, L., Marcos, S., Ravikumar, S., Thibos, L., Bradley, A., & Webster, M. (2010). Adaptation to astigmatic blur. Journal of Vision, 10(12), 22-22.
15. Bradley A., et al. "Effects of spherical and astigmatic defocus on acuity and contrast sensitivity: a comparison of three clinical charts." Optometry and vision science 68.6 (1991): 418-426
16. Remón L, Tornel M, Furlan WD. Visual acuity in simple myopic astigmatism: influence of cylinder axis. Optom Vis Sci. 2006 May;83(5):311-5. doi: 10.1097/01.opx.0000216099.29968.36. PMID: 16699444.
17. Hasegawa, Y., Hiraoka, T., Nakano, S., Okamoto, F., & Oshika, T. (2018). Effects of astigmatic defocus on binocular contrast sensitivity. PloS one, 13(8), e0202340.
18. Wolffsohn JS, Bhogal G, Shah S. Effect of uncorrected astigmatism on vision. J Cataract Refract Surg. 2011 Mar;37(3):454-60. doi: 10.1016/j.jcrs.2010.09.022. PMID: 21333869.
19. Black AA, Wood JM, Colorado LH, Collins MJ. The impact of uncorrected astigmatism on night driving performance. Ophthalmic Physiol Opt. 2019 Sep;39(5):350-357. doi: 10.1111/opo.12634. Epub 2019 Aug 4. PMID: 31378990.
20. Cox DJ, Banton T, Record S, Grabman JH, Hawkins RJ. Does correcting astigmatism with toric lenses improve driving performance? Optom Vis Sci. 2015 Apr;92(4):404-11. doi: 10.1097/OPX.0000000000000554. PMID: 25946099.
21. Verhoeff, F.H. 1900 The cause of a special form of monocular diplopia, Archives of Ophthalmology, vol 29, 565-572
22. Coffeen, Paul, and David L. Guyton. "Monocular diplopia accompanying ordinary refractive errors." American journal of ophthalmology 105.5 (1988): 451-459.
23. Apkarian, P., Tijssen, R., Spekreijse, H., & Regan, D. (1987). Origin of notches in CSF: optical or neural?. Investigative ophthalmology & visual science, 28(3), 607-612.

24. Atchison DA, Guo H, Charman WN, Fisher SW. Blur limits for defocus, astigmatism and trefoil. Vision Res. 2009 Sep;49(19):2393-403. doi: 10.1016/j.visres.2009.07.009. Epub 2009 Jul 23. PMID: 19631683.
25. Bullimore MA, Spooner G, Sluyterman G, Dishler JG. Correction of low levels of astigmatism. J Cataract Refract Surg. 2015 Aug;41(8):1641-9. doi: 10.1016/j.jcrs.2014.12.060. PMID: 26432121.
26. Kruse A, Løfstrøm T. How much visual benefit does an astigmat achieve being corrected with a toric correction? International Contact Lens Clinic 1996. 23(2):59-66. ISSN 0892-8967. doi: 10.1016/0892-8967(96)00006-5
27. Remón L, Monsoriu JA, Furlan WD. Influence of different types of astigmatism on visual acuity. J Optom. 2017 Jul-Sep;10(3):141-148. doi: 10.1016/j.optom.2016.07.003. Epub 2016 Sep 14. PMID: 27639497; PMCID: PMC5484781.
28. Richdale K, Berntsen DA, Mack CJ, Merchea MM, Barr JT. Visual acuity with spherical and toric soft contact lenses in low- to moderate-astigmatic eyes. Optom Vis Sci. 2007 Oct;84(10):969-75. doi: 10.1097/OPX.0b013e318157c6dc. PMID: 18049362.
29. Morgan PB, Efron SE, Efron N, Hill EA. Inefficacy of aspheric soft contact lenses for the correction of low levels of astigmatism. Optom Vis Sci. 2005 Sep;82(9):823-8. doi: 10.1097/01.opx.0000177792.62460.58. PMID: 16189492.
30. Read, S. A., Vincent, S. J., & Collins, M. J. (2014). The visual and functional impacts of astigmatism and its clinical management. Ophthalmic and Physiological Optics, 34(3), 267-294.
31. Bradley A., et al. "Effects of spherical and astigmatic defocus on acuity and contrast sensitivity: a comparison of three clinical charts." Optometry and vision science 68.6 (1991): 418-426.
32. Raasch, T. W. (1995). Spherocylindrical refractive errors and visual acuity. Optometry and Vision Science, 72(4), 272-275.
33. Ravalico, G., Parentin, F., & Baccara, F. (1999). Effect of astigmatism on multifocal intraocular lenses. Journal of Cataract & Refractive Surgery, 25(6), 804-807.
34. Ravikumar, S., Thibos, L. N., & Bradley, A. (2008). Calculation of retinal image quality for polychromatic light. Journal of the Optical Society of America A, 25(10), 2395-2407.
35. Berdahl, J. P., Hardten, D. R., Kramer, B. A., & Potvin, R. (2018). Effect of astigmatism on visual acuity after multifocal versus monofocal intraocular lens implantation. Journal of Cataract & Refractive Surgery, 44(10), 1192-1197.
36. Garzón, N., Poyales, F., de Zárate, B. O., Ruiz-García, J. L., & Quiroga, J. A. (2015). Evaluation of rotation and visual outcomes after implantation of monofocal and multifocal toric intraocular lenses. Journal of Refractive Surgery, 31(2), 90-97.

37. Hayashi K, Manabe S, Yoshida M, Hayashi H. Effect of astigmatism on visual acuity in eyes with a diffractive multifocal intraocular lens. J Cataract Refract Surg. 2010 Aug;36(8):1323-9. doi: 10.1016/j.jcrs.2010.02.016. PMID: 20656155.
38. Thibos LN, Hong X, Bradley A, Applegate RE. Metrics of optical quality of the eye. J Vis. 2004; 4: 1–15.
39. Thibos LN. Calculation of the geometrical point-spread function from wavefront aberrations. Ophthalmic Physiol Opt. 2019; 39: 232–44.
40. Thibos LN, Wheeler W, Horner D. Power vectors: an application of Fourier analysis to the description and statistical analysis of refractive error. Optom Vis Sci. 1997 Jun;74(6):367-75. doi: 10.1097/00006324-199706000-00019. PMID: 9255814.
41. Goodman, J. W. (2005), Introduction to Fourier Optics, 3rd ed., Roberts & Company.
42. Watson, A. B. (2015), Computing human optical point spread functions, Journal of Vision 15(2):26.
43. Atchison, D. A., & Smith, G. Optics of the Human Eye, Butterworth-Heinemann, 2000.
44. Bradley, A., Nam, J., Xu, R., Harman, L., & Thibos, L. (2014). Impact of contact lens zone geometry and ocular optics on bifocal retinal image quality. Ophthalmic and Physiological Optics, 34(3), 331-345.
45. Hayashi, K., Hayashi, H., Nakao, F., & Hayashi, F. (2000). Influence of astigmatism on multifocal and monofocal intraocular lenses. American journal of ophthalmology, 130(4), 477-482.
46. Zheleznyak, L., Kim, M. J., MacRae, S., & Yoon, G. (2012). Impact of corneal aberrations on through-focus image quality of presbyopia-correcting intraocular lenses using an adaptive optics bench system. Journal of Cataract & Refractive Surgery, 38(10), 1724-1733.

Appendix

Table 1. Zernike coefficients for a 22 y.o. subject, corresponding to a 4.8 mm pupil diameter. The label "variable" indicates that the value of these coefficients changed with the magnitude of cylinder (C2-2 and C22) and the plane of focus of the interval of Sturm (C20).

TERM	ABERRATION NAME	VALUE [µm]
C(0, 0)	Piston	0.0000
C(1,-1)	Vertical Tilt	0.0000
C(1, 1)	Horizontal Tilt	0.0000
C(2,-2)	Oblique Astigmatism	
C(2, 0)	Defocus	VARIABLE
C(2, 2)	Vertical Astigmatism	
C(3,-3)	Vertical Trefoil	-0.0203
C(3,-1)	Vertical Coma	0.1056
C(3, 1)	Horizontal Coma	-0.0572
C(3, 3)	Oblique Trefoil	0.0958

C(4,-4)	Oblique Quadrafoil	-0.0086
C(4,-2)	Oblique Sec. Astigmatism	-0.0042
C(4, 0)	Primary Spherical	0.0426
C(4, 2)	Vertical Sec. Astigmatism	0.0484
C(4, 4)	Vertical Quadrafoil	-0.0427
C(5,-5)	Pentafoil (Oblique)	0.0046
C(5,-3)	Secondary Trefoil (Oblique)	0.0231
C(5,-1)	Secondary Horizontal Coma	-0.0025
C(5, 1)	Secondary Vertical Coma	-0.0024
C(5, 3)	Secondary Trefoil (Vertical)	-0.0200
C(5, 5)	Pentafoil (Vertical)	0.0040
C(6,-6)	Hexafoil (Oblique)	0.0092
C(6,-4)	Secondary Quadrafoil (Oblique)	-0.0040
C(6,-2)	Tertiary Astigmatism (Oblique)	0.0066
C(6, 0)	Secondary Spherical Aberration	-0.0042
C(6, 2)	Tertiary Astigmatism (Vertical)	0.0102
C(6, 4)	Secondary Quadrafoil (Vertical)	0.0022
C(6, 6)	Hexafoil (Vertical)	0.0157

1 Consent to Publish declaration: not applicable.

2 Ethics and Consent to Participate declarations: not applicable